DOI: 10.1021/ma101157x

Macromolecules
ARTICLE

Revisiting the Conformation and Dynamics of DNA in Slitlike Confinement

Jing Tang,[†] Stephen L. Levy,[‡] Daniel W. Trahan,[†] Jeremy J. Jones,[†] Harold G. Craighead,[‡] and Patrick S. Doyle*,[†]

[†]*Department of Chemical Engineering, Massachusetts Institute of Technology, Cambridge, Massachusetts 02139, and* [‡]*School of Applied and Engineering Physics, Cornell University, Ithaca, New York 14853*

Received May 24, 2010; Revised Manuscript Received July 13, 2010

ABSTRACT: We experimentally investigated the equilibrium conformation and dynamics of single DNA molecules in slitlike nanochannels. We measured the in-plane radius of gyration ($R_{\|}$), diffusivity (D), and longest relaxation time (τ) of λ-DNA (48.5 kbp) as functions of the slit height using fluorescence microscopy. Our results show that the in-plane radius of gyration increases monotonically with decreasing slit height, in contrast to results from Bonthuis et al.[15] but in agreement with our simulations and those of other groups. In strong confinement (slit height <100 nm), the scaling of D, τ, and $R_{\|}$ with slit height does not show an evident change, suggesting that the transition from the de Gennes regime to the Odijk regime is gradual and broad.

1. Introduction

Although scaling theories for the properties of polymers under confinement have been proposed for years,[1−6] experimental investigations have only recently begun to be carried out. With the advances in microfabrication technologies, it is now possible to fabricate fluidic channels with well-defined geometries and characteristic dimensions on a scale of tens to hundreds of nanometers. Those devices, combined with fluorescence microscopy, have allowed the direct experimental observation of the conformation and dynamic behavior of highly confined polymers. Such knowledge can be used to not only test and refine existing theories of polymer physics but also guide the design and optimization of devices for the manipulation of biological macromolecules such as DNA.[7,8]

Slitlike confinement has served as a prominent platform in establishing scaling concepts for confined polymers.[1,2] Unlike the pseudobiaxial confinement in circular, square, or rectangular nanochannels, slitlike nanochannels offer a uniaxial confinement that constrains the polymer's orientational and translational degrees of freedom in only one dimension. The response of a polymer depends strongly on the strength of the confinement, and different regimes of confinement can be distinguished. Three competing length scales affect the final conformation of the chain: the 3D bulk radius of gyration $R_{g,bulk}$, the persistence length p of the polymer, and the height h of the confining slit. In weak confinement where $h \sim 2R_{g,bulk}$, the initial squeezing of the chain by the confining walls results in a decrease of the polymer's 3D size, as shown by Cordeiro et al.[9] using variational theory. Upon further confinement, the repulsive (excluded-volume) interactions between chain segments cause the chain to expand. In moderate confinement where $p \ll h < R_{g,bulk}$ (de Gennes regime), the dynamics of a polymer has been characterized by Brochard and de Gennes[1,2] using blob theory. The theory describes a confined polymer as a string of self-avoiding blobs with diameter equal to the slit height h and yields scaling predictions for the equilibrium size, diffusivity, and longest relaxation time of the polymer. The blob description of the chain breaks down as the slit height h approaches the persistence length p because the orientational and translational degrees of freedom become restricted (in the height dimension) even at the length scale of a single statistical segment. Instead, Odijk proposed[4−6] a deflection chain theory which argues that in such strong confinement the chain contour can be stored only through successive deflections of the chain from the wall.

A number of experimental[10−17] and simulation[18−23] studies have been conducted to quantitatively probe the equilibrium dynamics of polymer confined in nanoslits and test the above theories. Much progress has been made in understanding the polymer dynamics in the de Gennes regime (see reviews by Hsieh and Doyle,[24] Levy and Craighead,[25] and Graham[26]). Both experiments[10−13] and simulations[22] have provided consistent and compelling evidence suggesting that the framework of blob theory provides an adequate description of the conformation and dynamics of polymer under moderate slitlike confinement. Though, it has been shown[12] that the blobs are partial draining which is a minor correction to the assumptions of blob theory. Blob theory was shown to accurately predict the scalings of polymer's equilibrium size R with respect to chain length L_c and channel height h as well as the scalings of the diffusivity D and longest relaxation time τ with respect to L_c. The dependence of D and τ on the slit height h found in these studies, however, were slightly weaker than predicted by blob theory.[11,12] By assessing each individual assumption made in blob theory, Hsieh et al.[12] revealed that the origin of this discrepancy is solely due to the partial-draining nature of the blobs.

In contrast to the sound understanding gained for moderate confinement, a less clear picture has been established regarding the behavior of polymer in both weak confinement and strong confinement (Odijk's deflection chain regime), primarily because of the contradictory results presented in existing studies. In weak confinement, early studies by van Vliet and ten Brinke[18,19] using Monte Carlo simulations have shown a nonmonotonic behavior of the 3D radius of gyration of a self-avoiding walk confined in slits, in accord with predictions of Cordeiro et al.[9] Cifra and Bleha[20] also used Monte Carlo simulation to investigate a similar problem and characterized the behavior of both the mean-square

*Corresponding author. E-mail: pdoyle@mit.edu.

 Published on Web 08/05/2010

3D end-to-end distance ($\langle R_{3d}^2 \rangle$) and the projection of the end-to-end distance into the confining plane. Their results confirmed the initial dip of $\langle R_{3d}^2 \rangle$ upon slitlike confinement. However, the 2D projection of the end-to-end distance showed a monotonic increase from its bulk value with decreasing slit height. A similar trend of the 2D projections of both the end-to-end distance and maximum extension was reported in simulations performed by Hsu and Grassberger[21] and Chen et al.[22] Bonthuis et al.[15] recently measured the projected in-plane radius of gyration ($R_\parallel$) of DNA confined in nanoslits using fluorescence microscopy. Contrary to findings from simulations, the in-plane radius of gyration was larger than its bulk value at $h \approx 2R_{\parallel,\mathrm{bulk}}$ and was first reduced upon further confinement until $h \approx R_{\parallel,\mathrm{bulk}}/2$. Uemura et al.[17] also claimed to have experimentally observed the initial decrease of the 2D length of DNA molecules in weak slitlike confinement though the errors of their data overlap. In another experimental study, Lin et al.[16] investigated the 2D extension of DNA confined in nanoslits. Although the same DNA substrate was used and the range of slit height studied by Lin et al. is very similar to that in experiments of Bonthuis et al., the measured extension increased monotonically with decreasing slit height.

Disagreement also exists in studies attempting to probe the transition from the de Gennes regime to Odijk regime in nanoslits. The onset of the Odijk regime has been reported for square nanochannels by Reisner et al.[27] using single molecule DNA experiments. The measured scalings of DNA extension and relaxation time (determined from the stretch autocorrelation function) versus channel dimension h showed a strong discontinuity around $h \approx 100$ nm, about twice the DNA persistence length. The experimental scalings of both variables at $h < 100$ nm were found to be in agreement with Odijk's deflection chain theory. For nanoslits (channel width much larger than the polymer size), however, the applicability of the theory remains a question because the assumption of small fluctuations is not satisfied in the width dimension.[5] Several studies have suggested the transition between de Gennes regime and Odijk regime in nanoslits to be gradual and broad. Balducci et al.[11] measured the diffusivity of DNA in nanoslits over a wide range of slit height ($0.4 < R_{g,bulk}/h < 14$). No drastic change in the scaling of diffusivity with h was observed when the slit height approached the DNA persistence length. Strychalski et al.[14] also experimentally examined DNA diffusivity in nanoslits and extended the measurements into more shallow slits with height well below the DNA persistence length. No evident transition to the Odijk regime was identified even at a channel height of $h = 28$ nm, about half the persistence length. Instead, their diffusivity data followed a single power law over the full range of confinement studied, from 541 to 28 nm, and the extracted exponent was in good agreement with that reported by Balducci et al. Odijk[6] employed the Flory approach of minimizing the free energy of a confined polymer and proposed a scaling argument for the chain's equilibrium size. The scaling is identical with that predicted by blob theory as will be shown. Cifra et al.[23] performed Monte Carlo simulation of wormlike chain confined in slit. A rather mild change in the scaling of the end-to-end distance with channel height h was observed when h becomes smaller than the persistence length of the chain. On the other hand, Bonthuis et al.[15] measured the scaling of the in-plane radius of gyration and the relaxation time of DNA versus channel height in nanoslits. The scaling of both quantities displayed a sharp change at $h \approx 100$ nm, which Bonthuis et al. attribute to the onset of the Odijk regime. The in-plane radius of gyration beyond this transition channel height becomes independent of h, in disagreement with Odijk's prediction, and the relaxation time of DNA decreases with channel height. Lin et al.[16] also measured a plateau in the extension of DNA in nanoslits when the channel height is below the persistence length.

The purpose of the current study is to provide more insight into the conformation and dynamics of polymers within the two regimes of slitlike confinement where existing studies show inconsistent results. We use DNA as the model polymer and present experimental measurements of the in-plane radius of gyration, diffusivity, and the longest relaxation time of DNA confined in nanoslits with height varying from 8.5 μm to 32 nm. We also report the 3D conformation of DNA molecules in slitlike confinement obtained from Brownian dynamics simulations. There are two major focuses of this study: (1) investigating the response of DNA conformation to weak confinement and (2) probing whether a sharp transition between the de Gennes regime and Odijk regime exists in nanoslits.

2. Scaling Arguments for Polymer Dynamics in Nanoslits

In this section we briefly review the scaling predictions for polymers in slitlike confinement. We consider a linear polymer consisting of N statistical segments with length $2p$ in good solvent and confined in a slit with height h, where p is the persistence length.

2.1. Moderate Confinement: $p \ll h < R_{g,bulk}$. The behavior of a chain under moderate confinement where $p \ll h < R_{g,bulk}$ has been treated by de Gennes et al.[1,3] using blob theory. The theory assumes (1) the polymer can be modeled as a string of blobs with each blob having a diameter h, (2) statistical segments within each blob are not aware of the presence of the confinement and retain their 3D orientational and translational freedom as if they were in bulk, (3) the blobs follow a 2D self-avoiding walk, and (4) each blob is considered nondraining (i.e., segments within a blob interact hydrodynamically) while there are no hydrodynamic interactions between blobs.

From the Flory theory,[28] the bulk radius of gyration of the polymer follows the scaling $R_{g,bulk} \sim v^{1/5}p^{2/5}N^{3/5} \sim L_c^{3/5}(pw)^{1/5}$ where w is the effective diameter of the polymer, $v \approx wp^2$ is the excluded volume of a single segment, and $L_c = 2Np$ is the contour length. For a charged polymer such as DNA, the effective diameter w can deviate significantly from the bare diameter.[29] Using assumption (2) and the bulk scaling, one can estimate the number of polymer segments in each blob (g) as

$$g \sim h^{5/3}p^{-4/3}w^{-1/3} \tag{1}$$

The total number of blobs is thus given by $N_{blob} = N/g$. Assumption (3) allows one to extract the scaling of the equilibrium size of the chain (R):

$$R^2 \sim h^2 N_{blob}^{3/2} \sim L_c^{3/2}h^{-1/2}(pw)^{1/2} \tag{2}$$

The drag coefficient of the chain can be estimated using assumption (4):

$$\zeta_{chain} \sim \zeta_{blob}N_{blob} \sim \eta h N_{blob} \sim \eta L_c h^{-2/3}(pw)^{1/3} \tag{3}$$

where η is the solvent viscosity. The scaling of diffusivity can thus be written as

$$D \sim \frac{k_B T}{\zeta_{chain}} \sim \eta^{-1}L_c^{-1}h^{2/3}(pw)^{-1/3} \tag{4}$$

The spring constant H of a polymer near equilibrium has been shown[2,3] to be $H \sim k_B T/R^2$. The longest relaxation time τ is therefore given by

$$\tau \sim \frac{\zeta_{chain}}{H} \sim R^2\zeta_{chain} \sim \eta L_c^{5/2}h^{-7/6}(pw)^{5/6} \tag{5}$$

The assumptions made in the blob theory have been examined in detail in several experimental studies.[11,12] Only the assumption of nondraining blob was found compromised, which leads to deviations in the predicted h dependence of eqs 4 and 5.

2.2. Strong Confinement: $h < p$. In confinement with $h < p$, a less complete theoretical understanding of the static and dynamic properties of single polymer in nanoslits has been reached. Odijk[4] proposed a deflection chain theory to describe the behavior of a semiflexible polymer confined in a circular tube with the diameter much smaller than p. A new length scale was derived as the deflection length $\lambda \sim p^{1/3}h^{2/3}$, and the polymer chain was treated as a series of rigid rods of length λ that reflect off the channel boundary.[4] The deflection chain theory was further generalized for square and rectangular nanochannels;[5,6] it was suggested that the dynamics of polymer in strong confinement is greatly complicated by the formation of hairpins, and thus the transition from the de Gennes regime to the Odijk regime is nontrivial.

Although deflection chain theory has yielded close predictions of chain extensions in square and rectangular nanochannels comparing to experimental results,[8,27] it is still an open question whether the theory can be directly adapted to nanoslits with width much larger than p. Odijk[6] recently developed a scaling for the size of a highly confined chain in nanoslits using the Flory approach. He treated the polymer as L_c/λ rod segments squeezed into a 2D pancake with diameter R and height h. Because of the large channel width, the global persistence length[5] equals the chain persistence length p and the rod segments retain their orientational degree of freedom in directions parallel to the confining plane. Assuming the slit height is much larger than the effective width of the chain ($h \gg w$), the excluded volume of a single segment hence scales as $\beta \approx \lambda^2 w$, and the free energy of the chain is given by (eq 21 in ref 6)

$$\frac{F}{k_B T} \approx \frac{R^2}{L_c p} + \frac{\beta (L_c/\lambda)^2}{R^2 h} \tag{6}$$

The first term in eq 6 is the elastic energy needed to extend the chain to an extension of R, and the second term rises from the repulsive interactions (excluded-volume effects) of all L_c/λ chain segments. Minimization of F with respect to R yields

$$R^2 \sim (L_c p)\left(\frac{L_c w}{ph}\right)^{1/2} = {L_c}^{3/2} h^{-1/2} (pw)^{1/2} \tag{7}$$

The final result of eq 7 is identical to that of eq 2, suggesting that the scalings of R vs L_c and h do not change from the de Gennes regime to the Odijk regime. We note that the above derivation requires the second term in eq 6 to be greater than unity (i.e., the energy from the excluded-volume effects larger than $k_B T$). Substituting the result of eq 7 into eq 6, one obtains

$$\frac{\beta (L_c/\lambda)^2}{R^2 h} \sim \left(\frac{L_c w}{ph}\right)^{1/2} \tag{8}$$

Therefore, eq 7 is only valid when the excluded-volume parameter[6] $Z \sim L_c w/ph$ satisfies $Z > 1$. Otherwise, the behavior of the chain is effectively that of an ideal chain and its size remains constant as $R^2 \sim L_c p$.

Following the deflection chain picture and assuming no hydrodynamic interactions between chain segments, the drag coefficient of the chain can be estimated to be[11] $\zeta_{chain} \sim \zeta_{rod}(L_c/\lambda)$, where ζ_{rod} represents the drag coefficient of one rod segment. In a circular tube where hydrodynamic interactions are screened at a length scale equal to the tube diameter d_{tube}, ζ_{rod} is given by $\zeta_{rod} \sim n\lambda/\log(d_{tube}/d_h)$ with d_h the hydrodynamic diameter of the chain.[30] In nanoslits, however, the decay of the far-field velocity magnitude is not exponential,[31] and we write ζ_{rod} as $\zeta_{rod} \sim \eta\lambda/f(h)$ where $f(h)$ is a factor depending on the slit height. The diffusivity can thus be expressed as

$$D \sim \frac{k_B T}{\zeta_{chain}} \sim \eta^{-1} {L_c}^{-1} f(h) \tag{9}$$

Equations 4 and 9 suggest that the ${L_c}^{-1}$ dependence of D is expected for all slit heights, which was verified recently in single molecule DNA experiments.[14]

Polymer chains are not significantly elongated in nanoslits even when the slit height becomes smaller than the persistence length.[16,23] Therefore, one can assume the spring force remains linear near equilibrium and the longest relaxation time still keeps the same L_c dependence:

$$\tau \sim R^2 \zeta_{chain} \sim \eta {L_c}^{5/2} \tag{10}$$

3. Experiments

3.1. Channel and DNA Preparation. The nanoslits used in this study were fabricated from fused-silica wafers (Mark Optics) using two layers of contact photolithography and reactive ion etching (CHF_3/O_2) as described previously.[14] The device consisted of one 150 μm wide, 1 mm long nanoslit in the center and two 1 cm long deep regions on the sides of the slit. The channel depths were determined using a Tencor P-10 surface profiler and range from 32 to 560 nm. A 2 μm tall glass channel was donated by U.S. Genomics. A 8.5 μm tall channel was constructed in polydimethylsiloxane (PDMS, Sylgard 184, Dow Corning) using soft lithography on a silicon master (SU8-2 photoresist).

λ-DNA (48.502 kbp, New England Biolabs) suspended at a concentration of 0.69 μg/mL was stained with YOYO-1 (Invitrogen) dye at a base pair to dye ratio of 4:1 and allowed to sit at least overnight. DNA samples were diluted (2−10)-fold immediately before experiments to reach an optimal concentration for observation. Two types of experimental buffer were used: (1) 1.5 × TBE (270 mM Tris base, 270 mM boric acid, and 6 mM EDTA); (2) 1 × TE (10 mM Tris base and 1 mM EDTA), 50 mM NaCl. In both buffers an oxygen scavenger system consisting of 4 vol % β-mercaptoethanol (BME, Cabiochem), 12.5 mg/mL glucose (Mallinckrodt), 0.16 mg/mL glucose oxidase (Sigma), and 9.6 μg/mL catalase (Sigma) was incorporated. The buffer viscosities were determined to be 1.17 cP for the TBE buffer and 1.15 cP for the TE buffer at 22.5 °C by measuring the diffusivity of 0.925 μm polystyrene beads (Polysciences). The buffer ionic strengths were estimated to be 56.9 mM in the TBE buffer and 60.3 mM in the TE buffer.

3.2. Experimental Procedure. Nanoslits were filled via capillarity with a filtered solution of 50% ethanol and 50% deionized water. The device was then thoroughly rinsed with deionized water via application of potentials at the fluid reservoirs. The channel was further flushed with filtered 1 M NaOH for 4 min to remove any residual chemicals left from the fabrication process and rinsed again with water. Prior to each experiment, the channels were flushed with the experimental buffer for 1 h. DNA molecules were electrokinetically driven into the nanoslits using an electric field between 20 and 50 V/cm. A typical experiment involves identifying a molecule of interest, turning off the electric field, waiting for 1 min to allow the molecule to equilibrate from any deformation occurred while traveling in the channel, and then starting image acquisition. We used an inverted Zeiss Axiovert 200 microscope with a 100× NA 1.4

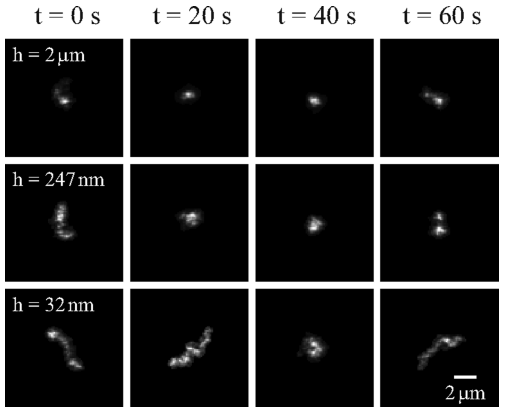

Figure 1. Snapshots of λ-DNA molecules confined in the 2 μm, 247 nm, and 32 nm tall nanoslits. For each nanoslit, images of a single molecule are shown, and the time interval between images is 20 s.

oil-immersed objective and an X-Cite 120 light source to observe single DNA molecules. Images were captured using a Hamamatsu EB-CCD camera (model 7190-21) and NIH image software at a rate of 30 frames/s for all experiments. 3600 frames (2 min) were collected for each molecule. Averages were taken over ensembles containing 30−70 different molecules per channel.

3.3. Data Analysis. We note that the DNA image taken from the fluorescence microscopy is a projection of the 3D molecule onto the $x-y$ plane (parallel to the confining channel walls) and thus does not explicitly contain information regarding the DNA size in the z-dimension (channel height dimension). The images were processed using custom-developed code in Interactive Data Language (IDL). A background image was subtracted from the image before the analysis (see Supporting Information for details). Figure 1 shows typical images (background subtracted) of λ-DNA in the channels. It is clearly seen that as the slit depth decreases, DNA molecule becomes more extended. We calculate the center-of-mass vector $\mathbf{r}_{cm}$ and the radius of gyration tensor $\mathbf{G}$ of the DNA in each frame:

$$\mathbf{r}_{cm}(t) = \frac{\sum \mathbf{r}(t) I(\mathbf{r}, t)}{\sum I(\mathbf{r}, t)} \tag{11}$$

$$\mathbf{G}(t) = \frac{\sum [\mathbf{r}(t) - \mathbf{r}_{cm}(t)][\mathbf{r}(t) - \mathbf{r}_{cm}(t)] I(\mathbf{r}, t)}{\sum I(\mathbf{r}, t)} \tag{12}$$

where the sum was taken over all pixels spanned by the molecule, $\mathbf{r}$ is the position vector, and $I(\mathbf{r},t)$ is the fluorescence intensity at position $\mathbf{r}$. The in-plane diffusivity D can be obtained from the mean-square displacement (MSD):

$$\mathrm{MSD}(\delta t) = \mathrm{MSD}_x(\delta t) + \mathrm{MSD}_y(\delta t) = 4D\delta t \tag{13}$$

where δt is the lag time, $\mathrm{MSD}_x(\delta t) = \langle [r_{cm,x}(t+\delta t) - r_{cm,x}(t)]^2 \rangle$, and $\mathrm{MSD}_y(\delta t) = \langle [r_{cm,y}(t+\delta t) - r_{cm,y}(t)]^2 \rangle$. Figure 2A and B show results of the center-of-mass trajectories and the MSD curves for λ-DNA in a 90 nm channel. In the absence of appreciable background flows, the center-of-mass trajectories yield a symmetric distribution, and the MSD values calculated for both the x-direction and y-direction agree well with each other.

The radius of gyration tensor $\mathbf{G}$ is related to the instantaneous size, shape, and orientation of the DNA. The 2D image of a molecule is described as an ellipse with the radii R_M and R_m of its major and minor principal axes given by

$$R_M = 2\sqrt{\lambda_1}, \quad R_m = 2\sqrt{\lambda_2} \tag{14}$$

where λ_1 and λ_2 ($\lambda_1 \geq \lambda_2$) are the eigenvalues of $\mathbf{G}$. The in-plane two-dimensional radius of gyration, denoted as $R_\parallel$, is given by the square root of the trace of $\mathbf{G}$ or

$$R_\parallel = \frac{1}{2}\sqrt{{R_M}^2 + {R_m}^2} \tag{15}$$

The angle between the major principal axis of the DNA and the x-axis is[32]

$$\theta(t) = \arctan\left(\frac{\lambda_1(t) - G_{xx}(t)}{G_{xy}(t)}\right), \quad -\frac{\pi}{2} < \theta < \frac{\pi}{2} \tag{16}$$

The longest rotational relaxation time τ_r and the longest stretch relaxation time τ_s are the characteristic times describing the slowest mode of the polymer's internal motion. τ_r and τ_s can be extracted by fitting a single-exponential function to the time autocorrelation function of $\theta(t)$ and $R_\parallel(t)$, respectively. The rotational autocorrelation function is defined as[12,32]

$$C_r(\delta t) = \frac{\langle (\theta(t+\delta t) - \theta_0)(\theta(t) - \theta_0) \rangle}{\langle (\theta(t) - \theta_0)^2 \rangle} \sim \exp(-\delta t/\tau_r) \tag{17}$$

where θ_0 is the equilibrium average of $\theta(t)$ and is taken to be zero in the calculation because the average orientation of a DNA is isotropic.[12] We have also verified this assumption from the experimental measurements (data not shown). The stretch autocorrelation function is defined as

$$C_s(\delta t) = \frac{\langle (R_\parallel(t+\delta t) - R_{\parallel,0})(R_\parallel(t) - R_{\parallel,0}) \rangle}{\langle (R_\parallel(t) - R_{\parallel,0})^2 \rangle} \sim \exp(-\delta t/\tau_s) \tag{18}$$

where $R_{\parallel,0}$ is the equilibrium average of $R_\parallel(t)$. We note that the rotational relaxation time obtained with our method is half of the true τ_r because the phase space is cut to half by defining the orientation of the major axis to be in between $-\pi/2$ and $\pi/2$. In this case τ_r and τ_s should equal to each other for a polymer chain in either a theta or good solvent.[28,33]

3.4. Effects of Photobleaching. Photobleaching of the fluorescent dye is always a practical concern in single molecule DNA experiments. The decreasing DNA fluorescent signal with time produces an apparent decay in the DNA size as measured by image analysis. For example, Figure 2C shows that the ensemble average fluorescence intensity of λ-DNA in a 90 nm tall slit drops by about 40% after 2 min of observation. Figure 2D displays the measured average in-plane radius of gyration $R_\parallel$ as a function of frame number (time). Despite the large degree of fluctuations, an overall decrease of $R_\parallel$ can be observed, as indicated by the black line which is a linear fit of the data. This decay in the measured $R_\parallel$ was observed for all slit heights. Photobleaching may also physically shorten the contour length of the DNA with time and thus change the dynamic properties of the molecule. The DNA is expected to diffuse and relax faster if it becomes shorter. Hence, we examine whether the DNA molecules remains intact by checking the time variation of both the diffusivity and relaxation time during the course of an experiment, as described by Hsieh et al.[12] For the diffusivity, we cut each individual movie into six submovies and compare the MSD curves from the ensemble average of the submovies. Since much better statistics are required to obtain accurate relaxation times, we divide the movies into two submovies and compare the corresponding autocorrelation curves. Figure 2E and F show results of such an analysis for λ-DNA in the 90 nm tall slit. The MSD curves of the six different ensembles plotted in Figure 2E show nearly exact superposition at small lag times. They deviate from each other at long lag times due to limited

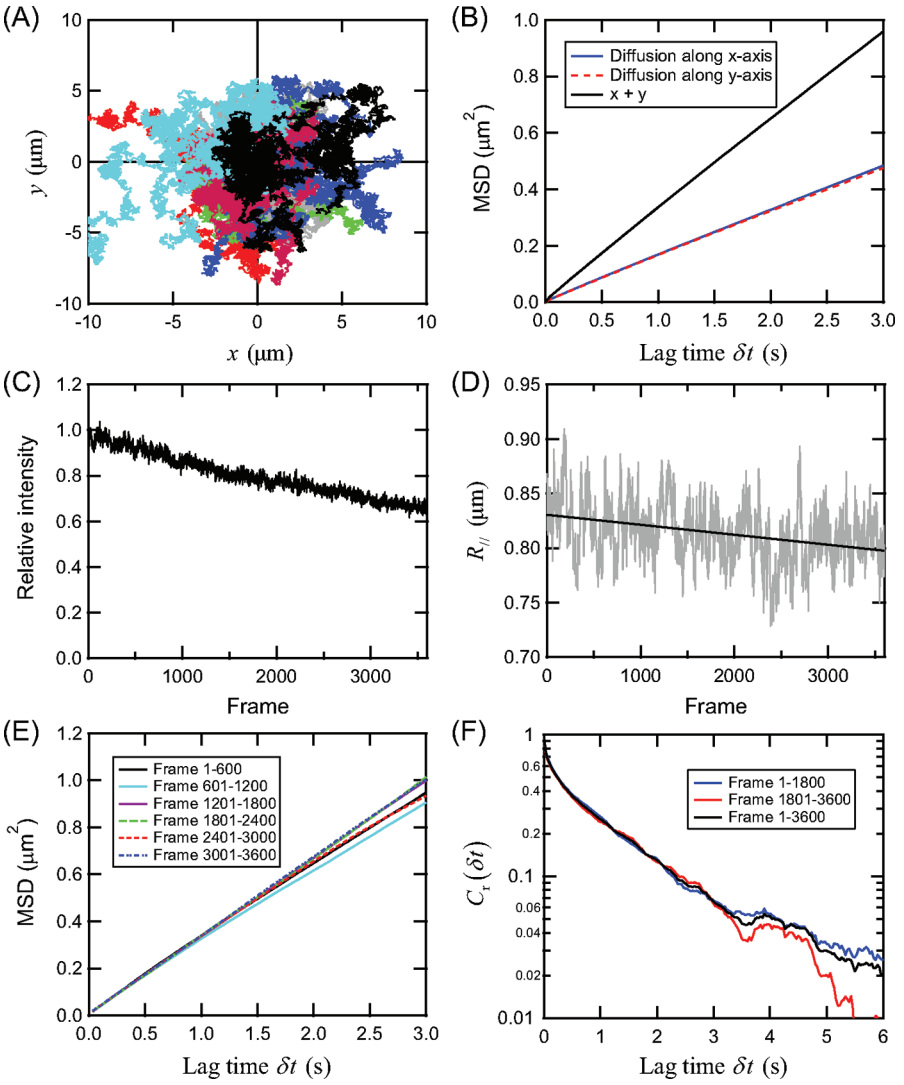

Figure 2. Summary of image analysis for λ-DNA in a 90 nm tall slit in the 1.5 × TBE buffer. (A) Center-of-mass trajectories for 35 λ-DNA molecules. (B) Mean-square displacement (MSD) as a function of lag time. The MSD along the *x*-axis and *y*-axis are also shown. (C) Evolution of the average fluorescence intensity of λ-DNA (normalized by the average intensity in the first frame) with frame number (1/30 s between consecutive frames). (D) Evolution of the average in-plane radius of gyration $R_{||}$ with frame number. The black line is a linear fit to the data showing an overall decrease of $R_{||}$ due to photobleaching. (E) Analysis of λ-DNA diffusion from difference time segments of the experimental movies. The MSD curves show good agreement at small lag times and fluctuate at long lag times due to limited statistics. (F) Analysis of the rotational autocorrelation function $C_r(\delta t)$ from different time segments of the experimental movies.

statistics, but no sign of systematic change is observed. Similar behavior of the rotational autocorrelation function was observed in Figure 2E, suggesting the physical properties of the DNA do not appreciably change over the course of an experiment.

3.5. Point Spread Function (PSF). The DNA image captured from the fluorescence microscopy is a convolution of the true image of YOYO-1 dyes with the point spread function (PSF) of the optical system.[34] The PSF causes the apparent size of the DNA to be larger than its actual value. To quantify this effect, we determine the in-plane PSF of our imaging system by measuring the intensity profile of 50 nm fluorescent polystyrene beads immobilized onto a glass coverslip. Figure 3 shows the typical image of a single 50 nm bead and its 2D intensity profile. We fit the image to a 2D Gaussian function given by[35]

$$I(x,y) = I_0 \exp\left(-\frac{(x-x_0)^2+(y-y_0)^2}{2{\sigma_{\mathrm{PSF}}}^2}\right) + B \qquad (19)$$

where I_0, x_0, y_0, σ_{PSF}, and B are fitting parameters. The standard deviation σ_{PSF} is determined to be about 190 nm. The optical

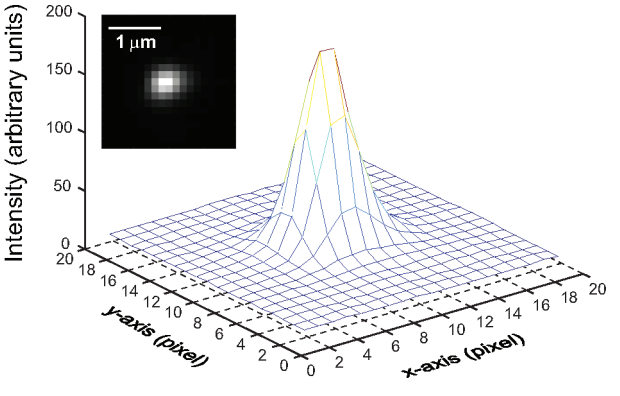

Figure 3. Typical image of a 50 nm fluorescent polystyrene bead under a 100× NA 1.4 objective and the corresponding 2D fluorescence intensity profile. One pixel corresponds to a length of 135 nm.

resolution σ_0, which is the full width at half-maximum of the point spread function, is $\sigma_0 = 2.355\sigma_{\mathrm{PSF}} \approx 450$ nm, significantly larger than the size of the beads used for the measurement. This value

is expected from the optical resolution of our microscope system of[34] ≈1.22 × excitation wavelength/NA (numerical aperture) ≈ 1.22 × 500 nm/1.4 ≈ 440 nm.

4. Results and Discussion

4.1. Conformation of DNA in Nanoslit. We measured the in-plane radius of gyration $R_{\|}$ of λ-DNA (using eq 15) from DNA images in slits with height from 8.5 μm to 32 nm. Because the values of $R_{\|}$ determined this way are consistently biased by both the point spread function and photobleaching of the dye, we only look at the qualitative aspect of the data and will not use them to develop the quantitative scaling relation between the DNA size and the slit height. A more precise estimation of the scaling exponent regarding the h dependence of DNA size can be inferred from the product of the DNA diffusivity D and rotational relaxation time τ_r, as will be discussed in a later section. Considering the experiments do not explicitly provide any information on the DNA conformation in the z-direction, we also performed Brownian dynamics simulations of a bead−spring chain confined in slitlike channels (see Supporting Information for details) to extract both the in-plane radius of gyration R and the true 3D radius of gyration R_g. The simulations were only carried out for channels taller than 90 nm as the spring force law used in the simulation model is expected to be not valid in channels with height smaller than the Kuhn length (~100 nm).[36]

The bulk in-plane radius of gyration $R_{\|,bulk}$ of λ-DNA was determined from its bulk diffusivity D_{bulk} using the relations $R_{g,bulk} = 0.203(k_BT/6^{1/2}\eta D_{bulk})$[33] and $R_{\|,bulk} = (2/3)^{1/2}R_{g,bulk}$, where $R_{g,bulk}$ is the bulk 3D radius of gyration. Since the measurement of the center of mass and thus the diffusivity is less sensitive to the point spread function and photobleaching, we expect the value of $R_{\|,bulk}$ evaluated this way to be more accurate than that directly measured from the DNA image. The measured bulk diffusivity of λ-DNA in the 1.5 × TBE buffer is $D_{bulk} = 0.45 \pm 0.02\ \mu m^2/s$, giving $R_{g,bulk} \approx 0.64\ \mu m$ and $R_{\|,bulk} \approx 0.52\ \mu m$. Bonthuis et al.[15] measured $R_{\|,bulk} \approx 0.84 \pm 0.1\ \mu m$ for λ-DNA in a solution of 10 mM Tris-EDTA and 50 mM NaCl. This value of $R_{\|,bulk}$ corresponds to $R_{g,bulk} \approx 1.03 \pm 0.12\ \mu m$, significantly larger than the value of $0.73 \pm 0.05\ \mu m$ reported by Smith et al.[37] for λ-DNA in a similar buffer (1 × TE, 10 mM NaCl).

Figure 4A shows the scaled ensemble average in-plane radius of gyration $\langle R_{\|}\rangle/R_{\|,bulk}$ of λ-DNA as a function of h measured both in experiments for 1.5 × TBE buffer and from Brownian dynamics simulations. The results reported by Bonthuis et al.[15] are also shown for comparison. The simulation results were calculated after the raw chain configurations were convoluted with the measured PSF and yield quantitative agreement with experiments. Both our experiments and simulations show monotonic increase of $\langle R_{\|}\rangle$ with decreasing h, in accord with previous simulations.[20−22] In the taller slits where $h > 2R_{g,bulk} \sim 1\ \mu m$, $\langle R_{\|}\rangle$ does not change significantly but stays nearly at a constant value which was slightly larger than the estimated $R_{\|,bulk}$ due to the point spread function. In contrast, the data of Bonthuis et al. exhibit vastly different behavior from bulk to $h \approx 400$ nm. The measured $R_{\|}$ is ~10% larger than $R_{\|,bulk}$ at $h = 1.3\ \mu m$, indicating there is an initial increase in $R_{\|}$ from bulk to this slit height. Further decrease in h leads to a compression of $R_{\|}$ until h reaches ~400 nm, below which $R_{\|}$ starts to grow again. We realize that Bonthuis et al. used a different approach to evaluate $R_{\|}$ instead of taking the ensemble average: they calculated $R_{\|}$ using eq 15 in which the values of R_M and R_m were determined from the peaks of their distributions. We have employed this method to analyze our experimental data, but the results show qualitatively the same trend with that of the ensemble average $R_{\|}$ (see Figure S2, Supporting Information). We notice that the data of $R_{\|}$ between our experiments and the study of Bonthuis et al. also show distinct behaviors in strong confinement ($h < 100$ nm). We will discuss these differences in a later section.

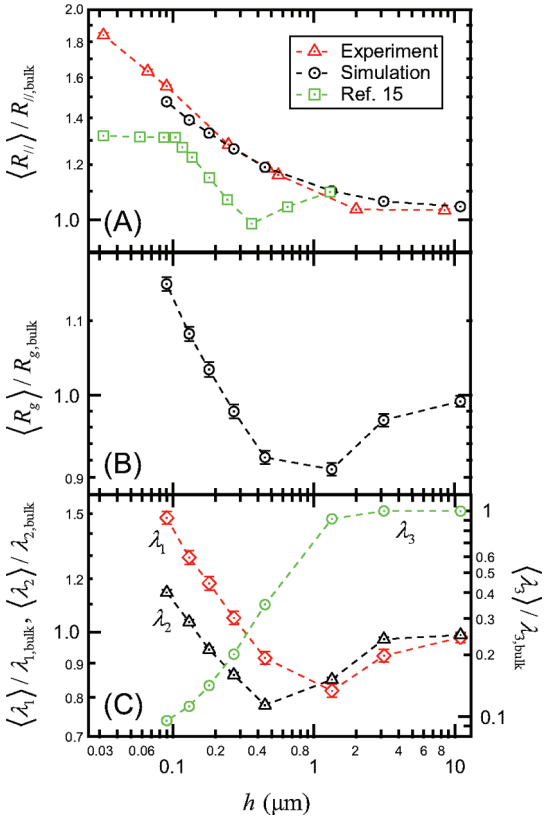

Figure 4. Dependence of different measurements of the DNA conformation on slit height h. (A) Ensemble average in-plane radius of gyration $R_{\|}$ (scaled by the estimated bulk value of 0.52 μm) measured experimentally in 1.5 × TBE buffer and determined from Brownian dynamics simulations. Error is less than the size of the symbols. The experimental errors do not include the possibly large systematic components induced by the PSF of the optical system and photobleaching of the YOYO-1 dye. The simulation results have been convoluted with the experimentally measured PSF (see Figure 3). Also shown are the results from Bonthuis et al.[15] measured using a slightly different method. (B) Ensemble average 3D radius of gyration R_g (scaled by its bulk value $R_{g,bulk}$) determined from simulations. (C) Ensemble average eigenvalues (λ_i, i = 1, 2, 3, all scaled by their bulk values) of the three principal axes of the 3D radius of gyration tensor determined from simulations.

Figure 4B shows the scaled 3D radius of gyration $\langle R_g\rangle/R_{g,bulk}$ determined from simulations without any PSF modification. It is clearly seen that R_g behaves differently from the projected 2D radius of gyration in slits with $h > 1\ \mu m$: while $\langle R_{\|}\rangle$ shows a mild increase, $\langle R_g\rangle$ decreases with h from its bulk value and displays a minimum at $h \approx 2R_{g,bulk}$. The trend of $\langle R_g\rangle$ and the location of its minimum observed in Figure 4B agree qualitatively with those reported by Cifra and Bleha.[20] Furthermore, we calculated the three eigenvalues (λ_i, i = 1, 2, 3, $\lambda_1 \geq \lambda_2 \geq \lambda_3$) of the 3D radius of gyration tensor from the simulations. The eigenvalues correspond to the square radii of the three principal axes of the radius of gyration tensor and can provide more details of the chain's 3D conformation. van Vliet and ten Brinke[18] have shown previously that the two larger eigenvalues λ_1 and λ_2 exhibit very similar behaviors with that of R_g, and the smallest eigenvalue λ_3 first remains constant for $h \gg 2R_{g,bulk}$ and decreases in further confinement. All these qualitative features have been

reproduced by our simulations, as can be seen from Figure 4C where results of $\langle\lambda_i\rangle/\lambda_{i,\mathrm{bulk}}$ are plotted against h.

We now point out that existing studies[9,18−20] that have reported an initial compression of the polymer coil by slitlike confinement all refer to the 3D size of the chain, and it is nonphysical for the projected 2D size to decrease with confinement. The 2D size of the chain is determined by the in-plane self-avoiding walk which depends upon the monomer density. A reduction in the z-dimension of the polymer by slitlike confinement will always increase the monomer density, and the resulting increased excluded-volume interactions will force the chain to expand in the $x-y$ plane. This monotonic increase of the 2D size of a confined polymer is verified by both our experiments and simulations as well as simulations from several other groups.[20−22] On the other hand, the change of the 3D polymer size is a competition between the swelling in the $x-y$ plane and the compression in the z-direction. As a coiled polymer becomes confined, the initial squeezing of the coil by the two confining planes does not significantly perturb the in-plane self-avoiding walk, and the decrease in the chain's z-dimension overwhelms the expansion in the $x-y$ plane, resulting in an overall reduction of the 3D coil size. Confinement also leads to reorientation of the principal axes of the chain.[18] Specifically, the two longer principal axes orient toward the $x-y$ plane and the shortest axis toward the z-direction. Before the two longer axes have considerably aligned, their radii are still affected by the z-dimension of the chain, and the initial decrease of $\langle\lambda_1\rangle$ and $\langle\lambda_2\rangle$ in weak confinement is again due to the compression of the chain in the z-direction.

4.2. Measuring the Longest Relaxation Time of DNA. We computed both the rotational autocorrelation function C_r and stretch autocorrelation function C_s from the time-sequence images of DNA to extract τ_r and τ_s, respectively. The standard deviation of the autocorrelation function is

$$\sigma_C = \frac{1}{\langle u^2\rangle}\sqrt{\langle u(t)^2u(t+\delta t)^2\rangle - \langle u(t)u(t+\delta t)\rangle^2} \qquad (20)$$

where u denotes either $(\theta-\theta_0)$ or $(R_\parallel - R_{\parallel,0})$. The standard deviation reaches its maximum value of 1 at sufficiently large lag time ($\delta t \gg \tau$) such that $u(t)$ and $u(t+\delta t)$ are uncorrelated. Therefore, we take the statistical noise to be $1/n^{1/2}$ for both C_r and C_s, where n is the total number of independent samples. The value of n was determined to be the product of the number of individual DNA movies collected for a given slit height and the number of independent samples in each movie taken as the length of the movie (2 min) divided by $3\tau_r$ (or $3\tau_s$).

Figure 5 shows examples of the autocorrelation functions measured for λ-DNA in a 247 nm and a 32 nm tall slits in the 1.5 × TBE buffer. The two horizontal lines indicate the corresponding statistical noise associated with these measurements. It is clearly seen that all four curves exhibit faster initial decay at small lag times due to contributions from higher order modes.[33] The decay gradually slows down and becomes single-exponential when the numerical values of these autocorrelation functions have decreased below about 0.3, indicating the slowest mode begins to dominate. The longest rotational relaxation time τ_r and the stretch relaxation time τ_s were determined by fitting the linear regions (in a semilog scale) of the corresponding autocorrelation curves. A wide linear region, starting from $C_r \sim 0.3$ and extending all the way down to statistical noise, can be identified from the two rotational autocorrelation curves, while a much smaller linear region exists in the stretch autocorrelation curves within the range $0.3 > C_s > 3\times$ noise. The slopes of the linear regions are similar between C_r and C_s for the same slit height. Two major reasons are responsible for the inferior quality of the stretch autocorrelation function.[12] First, the apparent decay of R induced by photobleaching (see Figure 2C) disrupts the linearity of C_s (in a semilog scale). In addition, the inability to accurately determine the mean equilibrium radius of gyration $R_{\parallel,0}$ from experiments often causes C_s to not decay to zero in the long time limit (see curve of C_s for the 247 nm tall slit in Figure 5). In contrast, photobleaching has a minimum effect on the measured orientation of DNA, and the value of θ_0 is analytically known to be zero, which has also been verified experimentally. As a result, the rotational relaxation time can be more accurately measured from experiments.

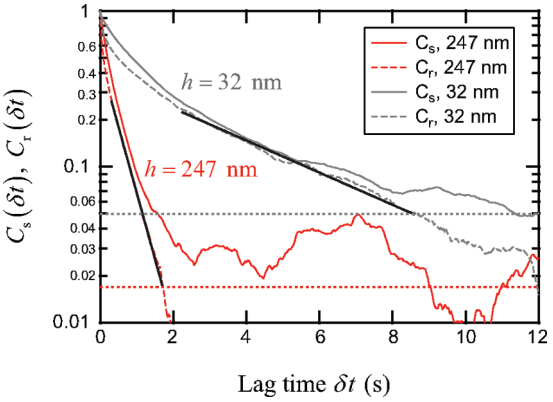

Figure 5. Curves of the rotational autocorrelation function C_r and the stretch autocorrelation function C_s versus the lag time δt for the 247 and 32 nm tall slits measured in the 1.5 × TBE buffer. The black solid lines are single-exponential fits to the rotational autocorrelation functions which were used to extract τ_r. The red and gray dotted horizontal lines indicate the statistical noises of these measurements for the 247 and 32 nm tall slits, respectively.

4.3. Static and Dynamic Scalings vs Channel Height. We have measured the diffusivity D, the longest rotational relaxation time τ_r, and the longest stretch relaxation time τ_s of λ-DNA in the 1.5 × TBE buffer in slits with heights of 2 μm, 560 nm, 471 nm, 247 nm, 90 nm, 66 nm, and 32 nm. We also performed the same measurements in the TE buffer in the 247 nm, 90 nm, and 66 nm tall slits to examine the possibility of any specific effects on the scaling of these dynamic properties from the interactions between DNA and the boric acid in the TBE buffer.[38]

Results of the dynamic properties of λ-DNA are summarized in Figure 6. Note that all the data have been corrected to correspond to a buffer viscosity of η = 1 cP using equations $D(1\text{ cP}) = D\eta$ and $\tau(1\text{ cP}) = \tau/\eta$. The errors do not include systematic components which are assumed to be small as these measurements are less affected by the point spread function and photobleaching. Figure 6A shows the DNA diffusivity as a function of slit height. The diffusivity data from 560 to 32 nm tall slit measured in the 1.5 × TBE buffer are well described by a single power law fit (by minimizing the value of chi-square) with an exponent of 0.49 ± 0.01. Both the values of diffusivity and its scaling with respect to h are in quantitative agreement with previous studies[12,14] (see Figure S3A, Supporting Information). The diffusivities measured in the TE buffer display similar slope (0.50 ± 0.04 determined from the three data points) with h, although their values are consistently larger than these in the TBE buffer under the same slit height. We do not observe any abrupt change in the scaling of diffusivity as the slit height becomes smaller than 100 nm, in accord with the results of Strychalski et al.[14]

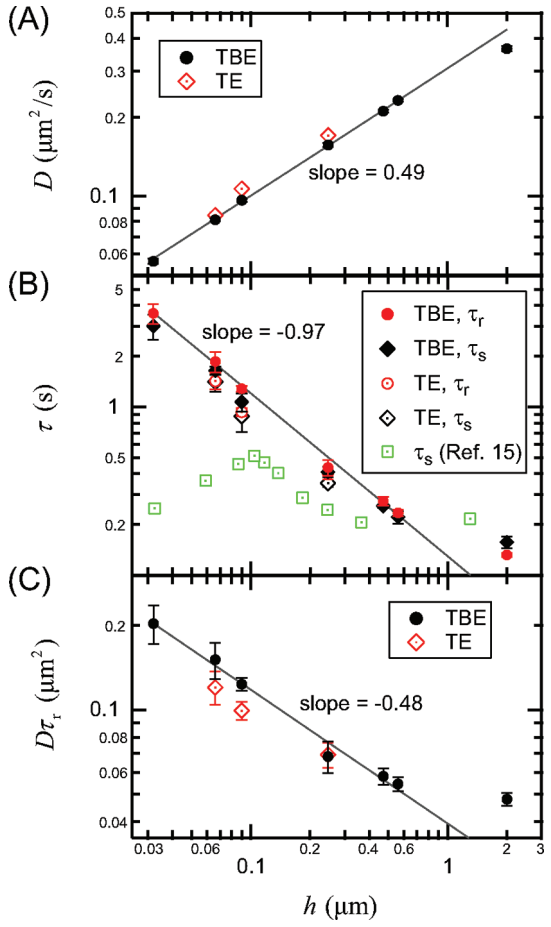

Figure 6. Dynamic properties of λ-DNA measured in both the 1.5 × TBE buffer and the TE buffer as functions of the slit height h. All data have been corrected to a buffer viscosity of 1 cP. Solid lines represent power law fits (by minimizing the value of chi-square) to the data (excluding the data for $h = 2\,\mu$m) from the TBE buffer. (A) Diffusivity. Error is less than the size of the symbols. Slope of the line is 0.49 ± 0.01. (B) The longest rotational relaxation time and stretch relaxation time. Solid line is a power law fit to the rotational relaxation time (for $h <$ 1 μm) in the TBE buffer. Slope of the line is -0.97 ± 0.03. Also shown are results of the stretch relaxation times reported by Bonthuis et al.[15] (C) Product of the diffusivity and the rotational relaxation time. Slope of the line is -0.48 ± 0.02.

Figure 6B shows the rotational relaxation time and stretch relaxation time against slit height h. Results of the stretch relaxation time of λ-DNA reported by Bonthuis et al.[15] are also plotted for comparison.[47] The measured rotational relaxation time τ_r and stretch relaxation time τ_s agree well with each other in both buffers, and they all show similar slope versus h. Switching the experimental buffer from TBE to TE leads to a decrease in both τ_r and τ_s (although the errors still overlap). Consistent with the scaling of diffusivity, no sudden change in the scaling of either τ_s or τ_r is seen for $h < 100$ nm. A single power law relation suffices to characterize all the relaxation time data for $h <$ 1 μm. The fitted scaling exponent is -0.97 ± 0.03 for τ_r and -0.94 ± 0.04 for τ_s in the TBE buffer, in quantitative agreement with the exponent of -0.92 ± 0.08 reported by Hsieh et al.,[12] who measured τ_r of λ-DNA in nanoslits with height from 760 to 92 nm (in the de Gennes regime). We have also compared the values of the rotational relaxation time with those reported by Hsieh et al., and the two sets of data agree well after viscosity and buffer ionic strength corrections (see Figure S3B, Supporting Information).

Before comparing the relaxation time data with these reported by Bonthuis et al., we first look at the scaling of $D\tau_r$, the product of diffusivity and rotational relaxation time. Although both D and τ_r depend on the drag coefficient of the chain ζ_{chain} (see eqs 4 and 5), their product is independent of ζ_{chain} and is only a function of chain size $D\tau_r \sim R^2$. Because both the diffusivity and rotational relaxation time can be more accurately determined from experiments than the in-plane radius of gyration, this quantity can be used as a better indicator of the DNA size. Figure 6C displays $D\tau_r$ as a function of h. It is seen that the scaling of $D\tau_r$ with h does not differ much between the two buffers. However, the values of $D\tau_r$ are smaller in the TE buffer, indicating that eliminating the boric acid from the buffer system reduces the size of DNA. This trend is in accord with the previous observations of larger diffusivity and shorter relaxation time in the TE buffer. As the two buffers bear similar ionic strength, the changes in these properties are most likely related to the interactions between DNA and the boric acid. A possible explanation for these differences is the higher charge density of DNA in the presence of boric acid[38] which can increase both the persistence length and effective width of DNA and thus alter the size and dynamic properties of the molecule toward the observed direction.[39] Nevertheless, the boric acid does not appear to have a strong effect on the scalings of DNA diffusivity, relaxation time, and their product with slit height.

The data of $D\tau_r$ from the TBE buffer also follow a single power law relation from $h = 560$ nm to $h = 32$ nm with a fitted slope of -0.48 ± 0.02. The same qualitative behavior is seen for the measured in-plane radius of gyration $R_{\parallel}$ (see Figure 4A). More importantly, the extracted scaling not only agrees with the blob theory prediction ($R^2 \sim h^{-0.5}$, eq 2) but also supports the scaling proposed by Odijk[6] ($R^2 \sim h^{-0.5}$, eq 7) for the deflection chain regime ($h < p$). We examine our experimental conditions to confirm that eq 7 is valid in our case. We estimate the persistence length and effective width of the DNA to be $p \approx 54$ nm (for unstained DNA) and $w \approx$ 6.6 nm in the 1.5 × TBE buffer.[29,39] The condition $h \gg w$ is satisfied even in the thinnest slit (32 nm tall) investigated. Also, the excluded-volume parameter $Z \sim L_c w/ph > (22000 \times 6.6)/(54 \times 100) \gg 1$ for $h < 100$ nm, indicating the repulsive interactions between deflection segments are important. *Overall, no sharp transition from the moderate confinement to strong confinement was identified in any of the experimental results.*

We observe two major discrepancies regarding the DNA size and relaxation time between the current study and experiments performed by Bonthuis et al. for 30 nm $< h <$ 400 nm. First, the values of τ_r and τ_s determined from our experiments are significantly larger (more than a factor of 2) than the results of Bonthuis et al. after viscosity correction. We notice that the number of YOYO-1 dye molecules used to stain a single λ-DNA was different in the two studies: a base pair to dye ratio of 4:1 was used in the current study while Bonthuis et al. used a ratio of 6:1. Intercalating dyes such as YOYO-1 are known to affect both the structural and mechanical properties of DNA.[40] It is generally assumed that the contour length of the DNA increases linearly with the amount of boundYOYO-1 up to about 35% at a saturating dye concentration of 1 dye per 4 base pairs.[27,41] We thus estimate that the contour length of λ-DNA to be ~10% longer in the current study than that in the study of Bonthuis et al. given the different staining ratio. For the persistence length of DNA, contradictory data exist regarding the effects of YOYO-1 binding. Several studies[42,43] used optical tweezers to probe the force−extension behavior of DNA and

suggested that the intercalation of YOYO-1 significantly reduces the DNA persistence length. On the other hand, Günther et al.[44] recently measured the force−extension curves of DNA using magnetic tweezers and found the persistence length of DNA to be rather independent of the staining ratio. Günther et al. claimed to have exclusively measured the entropic forces from bending fluctuations by suppressing the additional YOYO-1 intercalation which can occur at large applied forces.[42] Nevertheless, considering the small difference in the staining ratios used in the two studies, we do not expect the persistence length of the DNA to vary dramatically. For instance, we estimate the persistence length of λ-DNA to be only ~20% smaller in the current study using the relation between the DNA contour length and persistence length reported in Table 1 of ref 43. Note that the absolute values of the DNA persistence length in the current study and in the study of Bonthuis et al. are different from the data reported in ref 43 which were obtained in a buffer with a much higher ionic strength ($I \approx 160$ mM). However, we assume the relative ratio of the persistence length as a function of the contour length does not depend strongly on the ionic strength. From the relation $\tau \sim L_c^{5/2} p^{5/6}$ (see eq 5), the larger contour length and possibly smaller persistence length can make the relaxation time 5% higher in our experiments, which is far less than the difference seen in Figure 6B. In addition, the ionic strengths of both the TBE and TE buffer used in the current study are close to that used by Bonthuis et al. (10 mM Tris-EDTA, 50 mM NaCl, $I \approx$ 56 mM); the effects from the ionic strength induced changes in the persistence length and effective width of DNA[39] are thus expected to be minor. We do notice that Bonthuis et al. determined the stretch relaxation time by fitting the autocorrelation function C_s in the range of $1 > C_s > 0.1$. Since the decay of C_s at $C_s > 0.3$ still relies considerably on the higher order modes (see Figure 5), including this portion of the data in the fitting can significantly underestimate the longest relaxation time (see Table S2, Supporting Information), which we suspect is one of the main reasons for the vastly different relaxation times for the same DNA substrate and similar slit height between the two studies.

Second, the scalings of both $R_\parallel$ and τ_s with h reported by Bonthuis et al. show a strong discontinuity at $h \approx 100$ nm below which R becomes h-independent and τ_s starts to decrease with h. Our data do not shown these same trends. The stretch relaxation time measured by Bonthuis et al. is about the same for $h \approx 250$ nm and $h = 33$ nm. In contrast, we show a more than 8-fold increase in both τ_r and τ_s when the slit height is reduced from 247 to 32 nm. The corresponding autocorrelation functions also decay dramatically slower in the 32 nm tall slit, as can be seen in Figure 5. Bonthuis et al. did not report the diffusivity of λ-DNA. The distinct behaviors of DNA in the strong confinement is unlikely caused by the nanochannels as they were all fabricated from the same substrate with similar methods in both studies. The discrepancy persists when we performed the experiments in the TE buffer which has very similar composition with the buffer used by Bonthuis et al. It is possible that if the persistence length of the DNA in our experiments is significantly smaller than that in the study of Bonthuis et al., we might have not reached the regime where the slit height is much smaller than the persistence length and thus will not be able to observe the sharp transition. Given the fact that the transition was observed at $h \approx 100$ nm by Bonthuis et al. while we did not see any evident change in the scalings of DNA size, diffusivity, and relaxation time with h evenat $h = 32$ nm, the above postulation requires the persistence length of the DNA in our study to be at least $\sim (1 - 32/100) \approx 70\%$ smaller. However, as stated previously, we do not expect the persistence length of the DNA to be significantly different in the two studies. Currently the cause of the discrepancy still remains unclear.

5. Conclusion

In summary, we have experimentally investigated the equilibrium conformation and dynamics of single DNA molecules in slitlike nanochannels. We measured the in-plane radius of gyration, diffusivity, and longest relaxation time of λ-DNA (48.5 kbp) as functions of the channel height using fluorescence microscopy. The measured in-plane radius of gyration $R_\parallel$ displays a monotonic increase with decreasing channel height, in contrast to results from Bonthuis et al.[15] We further performed Brownian dynamics simulations and demonstrated that the behavior of the in-plane radius of gyration and the 3D radius of gyration is different in weak confinement where $h \sim 2R_{g,bulk}$, as suggested by previous simulations.[20] This finding stresses the importance to distinguish the true 3D conformation of a polymer and its 2D projection when comparing theories with experimental results which are usually 2D measurements. We also examined the scalings of the DNA size, diffusivity, and longest relaxation time versus slit height in slitlike channels with height from 2 μm to 32 nm. All three properties show a single power law scaling with h, indicating the transition from the de Gennes regime to Odijk's deflection chain regime should be broad and gradual. The measured scalings of diffusivity and relaxation time agree quantitatively with previous studies,[11,12,14] and the measured scaling of DNA size agrees with Odijk's recent scaling arguments,[6] namely that the h-dependence of the chain size does not change in the deflection chain regime. These results provide insight into the fundamental behavior of polymer under slitlike confinement and can be useful for the design of future processes aiming to utilize the capability of these ultrathin devices to drastically alter the conformation and dynamics of polymer chains. Finally, we remark that all the nanoslits investigated in our experiments are much taller than both the Debye screening length (~1 nm) and the effective width of the DNA. It is possible that further decrease in channel height can lead to considerable interactions between the local ionic environment near the negatively charged channel wall and the DNA backbone and thus induce other effects to DNA that are not considered in the current study.

Acknowledgment. The authors thank U.S. Genomics for the donation of the 2 μm tall channel used in this study. Funding was provided by Singapore-MIT Alliance for Research and Technology (SMART) and the National Science Foundation (CBET-0852235). Fabrication was performed at the Cornell NanoScale Science and Technology Facility, a member of the National Nanotechnology Infrastructure Network, and the Cornell Center for Materials Research, both of which are supported by the National Science Foundation.

Supporting Information Available: Description of the algorithm used to subtract the background of DNA images; description of the Brownian dynamics simulations; comparison of the in-plane radius of gyration $R_\parallel$ of λ-DNA evaluated using different methods; comparison of our data with several previous experimental studies; comparison of the longest relaxation times of of λ-DNA obtained by fitting the autocorrelation functions at C_r, $C_s < 0.3$ and from 0.1 to 1; movies of equilibrium single λ-DNA in a 247 nm tall (Movie S1) and a 32 nm tall (Movie S2) slits. This material is available free of charge via the Internet at http://pubs.acs.org.

References and Notes

(1) Brochard, F.; de Gennes, P. G. *J. Chem. Phys.* **1977**, *67*, 52.
(2) Brochard, F. *J. Phys.* (*Paris*) **1977**, *38*, 1285.

(3) Daoud, M.; de Gennes, P. G. *J. Phys.* (*Paris*) **1977**, *38*, 85.
(4) Odijk, T. *Macromolecules* **1983**, *16*, 1340.
(5) Odijk, T. *J. Chem. Phys.* **2006**, *125*, 204904.
(6) Odijk, T. *Phys. Rev. E* **2008**, *77*, 060901(R).
(7) Han, J.; Craighead, H. G. *Science* **2000**, *288*, 1026.
(8) Jo, K.; Dhingra, D. M.; Odijk, T.; de Pablo, J. J.; Graham, M. D.; Runnheim, R.; Forrest, D.; Schwartz, D. C. *Proc. Natl. Acad. Sci. U.S.A.* **2007**, *104*, 2673.
(9) Cordeiro, C. E.; Molisana, M.; Thirumalai, D. *J. Phys. II* **1997**, *7*, 433.
(10) Stein, D.; van der Heyden, F. H. J.; Koopmans, W. J. A.; Dekker, C. *Proc. Natl. Acad. Sci. U.S.A.* **2006**, *103*, 15853.
(11) Balducci, A.; Mao, P.; Han, J. Y.; Doyle, P. S. *Macromolecules* **2006**, *39*, 6273.
(12) Hsieh, C.-C.; Balducci, A.; Doyle, P. S. *Macromolecules* **2007**, *40*, 5196.
(13) Lin, P.-K.; Fu, C.-C.; Chen, Y.-L.; Chen, Y.-R.; Wei, P.-K.; Kuan, C. H.; Fann, W. S. *Phys. Rev. E* **2007**, *76*, 011806.
(14) Strychalski, E. A.; Levy, S. L.; Craighead, H. G. *Macromolecules* **2008**, *41*, 7716.
(15) Bonthuis, D. J.; Meyer, C.; Stein, D.; Dekker, C. *Phys. Rev. Lett.* **2008**, *101*, 108303.
(16) Lin, P.-K.; Lin, K.-H.; Fu, C.-C.; Lee, K.-C.; Wei, P.-K.; Pai, W.-W.; Tsao, P.-H.; Chen, Y.-L.; Fann, W. S. *Macromolecules* **2009**, *42*, 1770.
(17) Uemura, H.; Ichikawa, M.; Kimura, Y. *Phys. Rev. E* **2010**, *81*, 051801.
(18) van Vliet, J. H.; ten Brinke, G. *J. Chem. Phys.* **1990**, *93*, 1436.
(19) van Vliet, J. H.; Luyten, M. C.; ten Brinke, G. *Macromolecules* **1992**, *25*, 3802.
(20) Cifra, P.; Bleha, T. *Macromol. Theory Simul.* **1999**, *8*, 603.
(21) Hsu, H. P.; Grassberger, P. *J. Chem. Phys.* **2004**, *120*, 2034.
(22) Chen, Y. L.; Graham, M. D.; de Pablo, J. J.; Randall, G. C.; Gupta, M.; Doyle, P. S. *Phys. Rev. E* **2004**, *70*, 060901(R).
(23) Cifra, P.; Benkova, Z.; Bleha, T. *Faraday Discuss.* **2008**, *139*, 377.
(24) Hsieh, C.-C.; Doyle, P. S. *Korea-Aust. Rheol. J.* **2008**, *20*, 127.
(25) Levy, S. L.; Craighead, H. G. *Chem. Soc. Rev.* **2010**, *39*, 1133.
(26) Graham, M. *Annu. Rev. Fluid Mech.*, in press.
(27) Reisner, W.; Morton, K. J.; Riehn, R.; Wang, Y. M.; Yu, Z. N.; Rosen, M.; Sturm, J. C.; Chou, S. Y.; Frey, E.; Austin, R. H. *Phys. Rev. Lett.* **2005**, *94*, 196101.
(28) Rubinstein, M.; Colby, R. H. *Polymer Physics*; Oxford University Press: New York, 2003.
(29) Schellman, J. A.; Stigter, D. *Biopolymers* **1977**, *16*, 1415.
(30) Batchelor, G. K. *An Introduction to Fluid Dynamics*; Cambridge University Press: Cambridge, England, 1967.
(31) Liron, N.; Mochon, S. *J. Eng. Math.* **1976**, *10*, 287.
(32) Maier, B.; Rädler, J. O. *Macromolecules* **2000**, *33*, 7185.
(33) Doi, M.; Edwards, S. F. *The Theory of Polymer Dynamics*; Oxford University Press: New York, 1986.
(34) Hecht, E. *Optics*, 4th ed.; Addison Wesley: San Francisco, 2002.
(35) Zhang, B.; Zerubia, J.; Olivo-Marin, J. C. *Appl. Opt.* **2007**, *46*, 1819.
(36) Woo, N. J.; Shaqfeh, E. S. G.; Khomami, B. *J. Rheol.* **2004**, *48*, 281.
(37) Smith, D. E.; Perkins, T. T.; Chu, S. *Macromolecules* **1996**, *29*, 1372.
(38) Stellwagen, N. C.; Gelfi, C.; Righetti, P. G. *Biopolymers* **1997**, *42*, 687.
(39) Hsieh, C.-C.; Balducci, A.; Doyle, P. S. *Nano Lett.* **2008**, *8*, 1683.
(40) Lerman, L. S. *J. Mol. Biol.* **1961**, *3*, 18.
(41) Perkins, T. T.; Smith, D. E.; Larson, R. G.; Chu, S. *Science* **1995**, *268*, 83.
(42) Sischka, A.; Toensing, K.; Eckel, R.; Wilking, S. D.; Sewald, N.; Ros, R.; Anselmetti, D. *Biophys. J.* **2005**, *88*, 404.
(43) Murade, C. U.; Subramaniam, V.; Otto, C.; Bennink, M. L. *Nucleic Acids Res.* **2010**, *38*, 3423.
(44) Günther, K.; Mertig, M.; Seidel, R. *Nucleic Acids Res.* **2010**, DOI: 10.1093/nar/gkq434.
(45) Randall, G. C.; Doyle, P. S. *Phys. Rev. Lett.* **2004**, *93*, 058102.
(46) Fang, L.; Hu, H.; Larson, R. G. *J. Rheol.* **2005**, *49*, 127.
(47) We note that Bonthuis et al.[15] referenced a previous study from our group[45] for the bulk relaxation λ-DNA (0.2 s) which was in fact measured in a 2 μm tall channel, where $2R_{g,bulk}/h \sim 1$. This value is about twice the true bulk relaxation time of λ-DNA in a 1 cP buffer (0.1 s).[46]